Mössbauer Effects and Magnetic Properties of Mixed Valent Europium Sulfide, EuPd₃S₄

Makoto Wakeshima, Yoshihiro Doi, and Yukio Hinatsu

Division of Chemistry, Graduate School of Science, Hokkaido University, Sapporo 060-0810, Japan

and

Nobuyuki Masaki

Japan Atomic Energy Research Institute, Tokai-mura, Ibaraki 319-1195, Japan

$EuPd_3S_4$ with a $NaPt_3O_4$-type structure was investigated by X-ray diffraction, ^{151}Eu Mössbauer spectroscopy, magnetic susceptibility, and specific heat measurements. In this compound, Eu^{2+} and Eu^{3+} ions exist in the ratio of ca. 1:1. The Debye temperatures of Eu^{2+} and Eu^{3+} were determined to be 195 and 220 K, respectively. The isomer shift of Eu^{2+} in this $EuPd_3S_4$ at 300 K is largest among Eu^{2+} sulfides because of the compression effect of the Eu^{2+} sites. The temperature dependence of the isomer shifts suggests that a hopping of the electron between Eu^{2+} and Eu^{3+} occurs in $EuPd_3S_4$. The Eu^{2+} ion was found to be in the antiferromagnetic state below 3 K from both the magnetic susceptibility and specific heat measurements. © 2001 Academic Press

INTRODUCTION

Rare earth palladium sulfides, RPd_3S_4 (R = rare earths), have been reported to crystallize in an ideal $NaPt_3O_4$-type structure with space group $Pm3n$ (1–4). The schematic structure of RPd_3S_4 is illustrated in Fig. 1. Some of these compounds were reported to be metallic and they showed paramagnetic behavior down to 4.2 K. However, the R ions in RPd_3S_4 are expected to undergo magnetic ordering at low temperatures by a RKKY-type or Kondo-type interaction via conduction electrons. Earlier we reported that $CePd_3S_4$ and $GdPd_3S_4$ showed a ferromagnetic transition at 5.8 K and an antiferromagnetic transition at 5.8 K, respectively (5). The R ions occupy the cubic symmetric site (a point group T_h) being coordinated to eight sulfur ions as shown in Fig. 1 and the ground states of the R ions are predicted to be in the highly degenerated states. In these compounds, the orbital degeneracy of the ground state of the R ions can be removed by such interactions as a cooperative Jahn–Teller effect or an ordering of quadru-

poles. Recently, Abe *et al.* (6) confirmed that the R ions from Ce to Yb, except for Tm, had degenerated ground states and some R ions indicated quadrupolar pair interactions from measurements of the electrical conductivity, magnetic susceptibility, and specific heat. In $TmPd_3S_4$, Jahn–Teller-like phase transition occurred around 200 K (7).

In these compounds, the Eu and Yb ions are in the mixed valence state in which the divalent and trivalent states coexist while the other R ions are in the trivalent state (4, 6). We have been interested in the electronic state of Eu ions in $EuPd_3S_4$. For investigation of a mixed valence state of Eu ions, ^{151}Eu Mössbauer spectroscopy is very useful since the different shielding of the closed s electrons by the $4f^6$ and $4f^7$ configurations results in an increase of the s-electron density at ^{151}Eu nucleus in Eu^{3+} compound compared to that in Eu^{2+} compound. The difference in the Mössbauer absorption energy between Eu^{2+} and Eu^{3+} is ca. 14 mm s^{-1}, which is greater than the natural line width ~ 1.31 mm s^{-1}, and thus the valence state of Eu ion can be considered exactly. In order to obtain information on the magnetic properties of $EuPd_3S_4$ and to elucidate the electronic state of Eu ions, we have measured the Mössbauer spectra, the magnetic susceptibilities, and the specific heat, which are reported in this paper.

EXPERIMENTAL

The sample was prepared by a solid-state reaction. The calculated amounts of europium sulfide (EuS), palladium powder, and sulfur were mixed in an agate mortar. The mixture was put into a quartz tube, evacuated, and sealed. Subsequently, the ampoule was heated at 1173 K. The product was sintered repeatedly until the $NaPt_3O_4$-type phases were confirmed with no trace of the other phase by
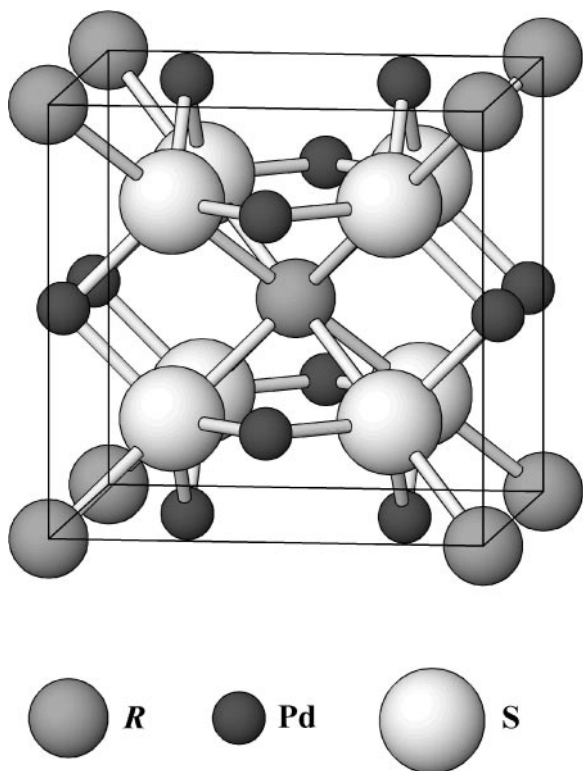
FIG. 1. Schematic structure of RPd$_3$S$_4$ (R = rare earth elements).

a powder X-ray diffraction measurement at room temperature.

A low-temperature powder X-ray diffractometry was carried out with a Rigaku RINT2200 diffractometer employing Cu$K\alpha$ radiation monochromatized with curved pyrolytic graphite in order to examine the temperature dependence of the lattice parameters. This diffractometer was equipped with a variable temperature cryostat system CryoMini (Iwatani Industrial Gases Co.). The program RIETAN97 (8) was used for refining the lattice parameters.

The ^{151}Eu Mössbauer spectrum was measured at 10, 100, 200, and 300 K with a Mössbauer spectrometer VT-6000 (Laboratory Equipment Co.) using a radiation source ^{151}SmF$_3$ (1.85 GBq). The sample lapped in an aluminum foil was cooled down to each temperature by using a variable temperature cryostat system CryoMini (Iwatani Industrial Gases Co.). The spectrometer was calibrated using α-iron at room temperature and the isomer shift was determined relative to the shift of europium fluoride (EuF$_3$).

Magnetic susceptibilities were measured using a SQUID magnetometer (Quantum Design, Model MPMS) from 1.8 to 300 K. The applied magnetic field was 0.1 T. In the neighborhood of the magnetic transition, the magnetic susceptibility was measured under both zero-field-cooled condition (ZFC) and field-cooled condition (FC) with a field of 5 mT. The field dependence of magnetization was measured

at 1.8 and 4.5 K by changing the applied magnetic field between -5 and 5 T.

The specific heat measurement was carried out using a relaxation technique supplied by the commercial specific heat measurement system (Quantum Design, PPMS) in the temperature range from 1.8 to 300 K. The sample in the form of pellet (~ 7 mg) was mounted on an aluminum plate with apiezon for better thermal contact.

RESULT AND DISCUSSION

Crystal Structure

The X-ray diffraction patterns of EuPd$_3$S$_4$ showed that this compound crystallizes in a cubic structure with space group $Pm3n$. No phase transition occurred in the temperature range from 10 to 300 K. Figure 2 shows the lattice parameters and cell volumes as a function of temperature. The lattice parameters increase monotonously with temperature above 50 K but the lattice parameters became constant below 50 K since the coefficient of thermal expansion is proportional to T^3 at low temperatures. The linear coefficient of thermal expansion between 50 and 300 K is calculated to be 5.2×10^{-6} K^{-1} in the unit of $\Delta a/a$ (15.5×10^{-6} K^{-1} in the unit of $\Delta V/V$). This value is reasonable in comparison with those of other sulfides, e.g., 11.9×10^{-6} K^{-1} for CaY$_2$S$_4$ in the unit of $\Delta V/V$ [9], 6.5×10^{-6} K^{-1} for ZnGa$_2$S$_4$, 6.8–8.4×10^{-6} K^{-1} for spinel-type sulfides, and 12.9–17.8×10^{-6} K^{-1} for Th$_3$P$_4$-type sulfides in the unit of $\Delta a/a$ (10). In this compound, the Eu^{2+} and Eu^{3+} ions occupy one equivalent site (2a site) in the ratio of ca. 1:1 (3). If the ratio of the Eu^{2+} and Eu^{3+} ions is changed by 1%, the variation of cell volume, which is

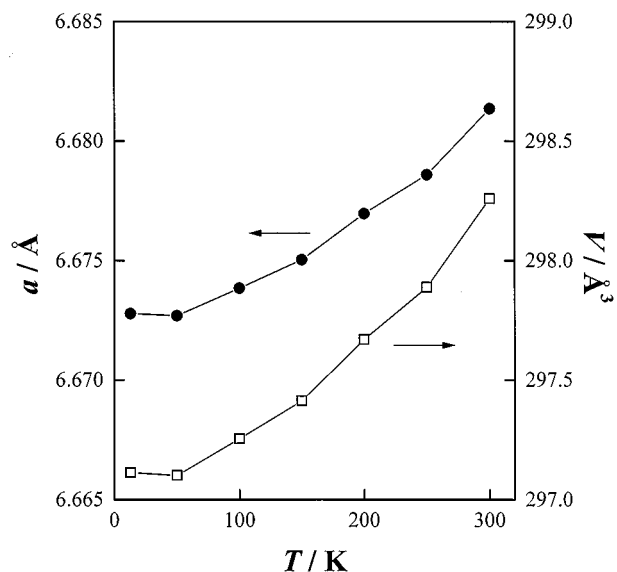FIG. 2. Temperature dependence of the lattice parameter and the cell volume for EuPd$_3$S$_4$.

proportional to the third power of the average Eu–S bond length, is calculated to be ca. 0.2% by Shannon's ionic radii (1.39 Å for Eu^{2+} and 1.206 Å for Eu^{3+} (11)). Thus, the absence of anomaly in the cell volume vs temperature curve in Fig. 2 indicates that there is no, or a very slight, change in the ratio of Eu^{2+} and Eu^{3+}.

Mössbauer Spectroscopy

Figure 3 shows the ^{151}Eu Mössbauer spectra of EuPd₃S₄ at 10, 100, 200, and 300 K. Two absorption peaks appeared at ca. −11 and 0 mm s^{-1} in these spectra, indicating that the Eu ions are in both the divalent and the trivalent state. In EuPd₃S₄, the Eu ions occupy the 2a site (space group *Pm3n*) with a cubic point group T_h, and one can expect nonexistence of an electric quadrupole interaction between the electron field gradient and the electric quadrupole moment. Therefore, each of the peaks corresponding to the divalent and trivalent Eu ions can be fitted with a single Lorentzian. The refined isomer shifts δ, the full linewidths at half maximum Γ, and the peak intensities I are listed in Table 1.

Figure 4 shows the temperature dependence of the absorption area of the intensity curves of the Eu^{2+} and Eu^{3+} ions. Both intensities decrease monotonously with increasing temperature and the decrease for Eu^{2+} is larger than that for Eu^{3+}. This difference may be due to a small difference in the Debye–Waller factors between Eu^{2+} and Eu^{3+}. The area of the intensity curve is proportional to the recoil-free fraction. On the assumption that the valence fluctuation

TABLE 1
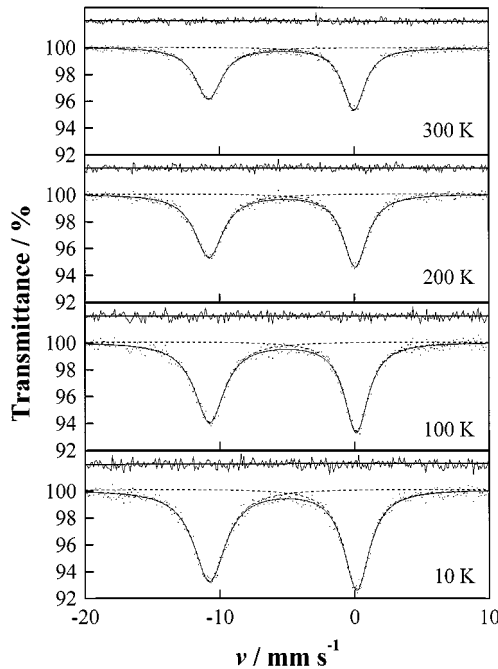**Absorption Intensity Parameters of Mössbauer Spectra for EuPd₃S₄**

		δ (mm s^{-1})	Γ (mm s^{-1})	I (%)	n (%)
300 K	Eu^{2+}	−10.73(2)	2.61(7)	3.56(6)	49.7
	Eu^{3+}	0.01(2)	2.24(5)	4.19(6)	50.3
200 K	Eu^{2+}	−10.76(2)	2.58(5)	4.73(6)	51.3
	Eu^{3+}	0.07(1)	2.16(4)	5.45(6)	48.7
100 K	Eu^{2+}	−10.76(2)	2.74(6)	6.03(7)	53.1
	Eu^{3+}	0.14(2)	2.17(4)	6.74(8)	46.9
10 K	Eu^{2+}	−10.78(1)	2.88(4)	6.85(5)	53.8
	Eu^{3+}	0.15(1)	2.28(3)	7.42(6)	46.2

Note. δ, isomer shift; Γ, full linewidth at half maximum; I, peak intensity; n, relative area intensity.

does not occur below 300 K, as evident from the result of X-ray diffraction measurements, the Debye temperatures for Eu^{2+} and Eu^{3+} are estimated from the recoil-free fraction. The recoil-free fraction is represented by (14)

$$f = \exp\left[\frac{-6E_R}{k\Theta_D}\left\{\frac{1}{4} + \left(\frac{T}{\Theta_D}\right)^2 \int_0^{\Theta_D/T} \frac{x\,dx}{(e^x - 1)}\right\}\right], \quad [1]$$

where k is the Boltzmann's constant, Θ_D is the Debye temperature, and E_R is the free-atom recoil energy. The theoretical curves with $\Theta_D = 195$ K (solid line in Fig. 4) and $\Theta_D = 220$ K (broken line in Fig. 4) using Eq. [1] are in good agreement with the experimental data for Eu^{2+} and Eu^{3+}, respectively.

In EuPd₃S₄ compound, the isomer shifts of Eu^{2+} and Eu^{3+} at 300 K are determined to be −10.73(2) and

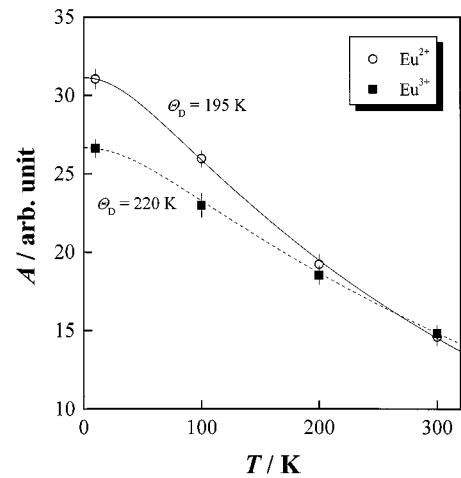**FIG. 3.** ^{151}Eu Mössbauer spectra of EuPd₃S₄ at 10, 100, 200, and 300 K.

FIG. 4. Temperature dependence of the absorption area of intensities of EuPd₃S₄; the solid line is the theoretical curve ($\Theta_D = 195$ K) normalized to $A(Eu^{2+})$ at 10 K and the broken line is the theoretical curve ($\Theta_D = 220$ K) normalized to $A(Eu^{3+})$ at 10 K.

0.01(2) mm s^{-1}, respectively. This value for Eu^{2+} is the largest among the known isomer shifts for Eu^{2+} sulfides. On the other hand, the isomer shift for Eu^{3+} is relatively small in comparison with those for other Eu^{3+} sulfides. The isomer shift is given by (14)

$$\delta = \frac{4\pi}{5} Ze^2 R^2 \left(\frac{\Delta R}{R}\right) \{|\psi_A(0)|^2 - |\psi_S(0)|^2\}, \quad [2]$$

where $|\psi_A|$ and $|\psi_S|$ are the electron charge densities at the nuclei of the absorber and the source, respectively, R is the average radius of the nuclei in the ground state and the excited state, and ΔR is the difference between the radii in the ground state and the excited state. Since the difference $\Delta R/R$ has a positive value for the ^{151}Eu nucleus (12), the largest value of the isomer shift for Eu^{2+} suggests that the electron density at the ^{151}Eu nucleus is the highest among those of the Eu^{2+} sulfides reported until now. In RPd$_3$S$_4$, the R–S bond lengths for lighter rare earths are shorter than the bond lengths calculated from Shannon's radii (4). In the case of the mixed valent europium compound EuPd$_3$S$_4$, X-ray diffraction measurement shows that the mean Eu–S bond length (2.893 Å at 300 K) is shorter than the calculated Eu^{3+}–S^{2-} length (2.906 Å), although it is expected to be longer than the calculated Eu^{3+}–S^{2-} length. Therefore, we believe that the Eu^{2+}–S^{2-} length in this EuPd$_3$S$_4$ should be shorter than the 'normal' Eu^{2+}–S^{2-} lengths. In divalent europium compounds, it is known that the isomer shifts increase monotonously with decreasing the Eu^{2+}–S^{2-} length (13). This correlation indicates that the shorter Eu^{2+}–S^{2-} length in EuPd$_3$S$_4$ increases the electron density at the ^{151}Eu nuclei.

The large isomer shift of Eu^{2+} arises from the following two mechanisms, the pressure effect and the concentration effect. The pressure effect for an increase of the isomer shift can be explained by the compression of the closed inner shells (5s shell) and the s-like part of the valence electrons, and the promotion of a 4f electron into the conduction band (14). On the other hand, the concentration effect was investigated by varying the concentration of Eu ions in the Ca$_{1-x}$Eu$_x$F$_2$ and Ca$_{1-x}$Eu$_x$S systems (15). In these systems, the substitution of Ca^{2+} by Eu^{2+} is expected to increase the isomer shift of Eu^{2+} because the size of the Ca^{2+} ion is smaller than that of Eu^{2+}. However, the isomer shift decreases with decreasing Eu^{2+} concentration in Ca$_{1-x}$Eu$_x$S in the range of $x < 3.5\%$, while it increases with decreasing Eu^{2+} concentration in Ca$_{1-x}$Eu$_x$F$_2$. Wickman et al. explained this behavior by the change in the $p_\pi \rightarrow 5d\ t_2$ type donation which leads to opposite trends in the isomer shift for the octahedral coordination in CaS and the cubic coordination in CaF$_2$ (15). The Eu^{2+} ion in EuPd$_3$S$_4$ has the eight-fold cubic coordination and the concentration effect for EuPd$_3$S$_4$ should be the same as that for Ca$_{1-x}$Eu$_x$F$_2$; therefore the isomer shift of Eu^{2+} in EuPd$_3$S$_4$ is expected to

be larger than that of a "pure" Eu^{2+} compound. Thus, such a concentration effect may contribute to an increase of the Eu^{2+} isomer shift in addition to the pressure effect. To discuss the large Eu^{2+} isomer shift and the small Eu^{3+} isomer shift of EuPd$_3$S$_4$ measured at room temperature, the following temperature dependence of the isomer shifts must be taken into account.

Figure 5 shows the temperature dependence of the isomer shifts of Eu^{2+} and Eu^{3+}. The isomer shift of Eu^{3+} decreases with increasing temperature. This decrease should be attributable to the second-order Doppler (SOD) shift and to the change in the electron density at the ^{151}Eu nuclei. According to the Debye model, the temperature dependence of the second-order Doppler shift $\Delta\delta_{SOD}$ can be expressed by the following equation (16),

$$\Delta\delta_{SOD} = \frac{-9kT}{2Mc} \left\{\frac{1}{8}\frac{\Theta_D}{T} + \left(\frac{T}{\Theta_D}\right)^3 \int_0^{\Theta_D/T} \frac{x^3\,dx}{(e^x - 1)}\right\}, \quad [3]$$

where M and c are the mass of isotope and the speed of light, respectively. The difference in the isomer shifts between 10 and 300 K (0.14 mm s^{-1}) is larger than the second-order Doppler shift of ^{151}Eu calculated from Eq. [3] as shown in Fig. 5 (0.06 mm s^{-1}). This difference may be due to the decrease of the electron densities at the nuclei by the lattice expansion. The contribution of the thermal expansion to the isomer shift is estimated to be ca. 0.04 mm s^{-1} from the correlation between the Eu^{2+}–S^{2-} bond length and the isomer shifts (13). Thus, the sum of the second-order Doppler shift and the shift due to the thermal expansion is still smaller than the difference in the isomer shifts between 10 and 300 K.

As shown in Fig. 5, the isomer shift of Eu^{2+} seems to increase with increasing temperature, and that of Eu^{3+}
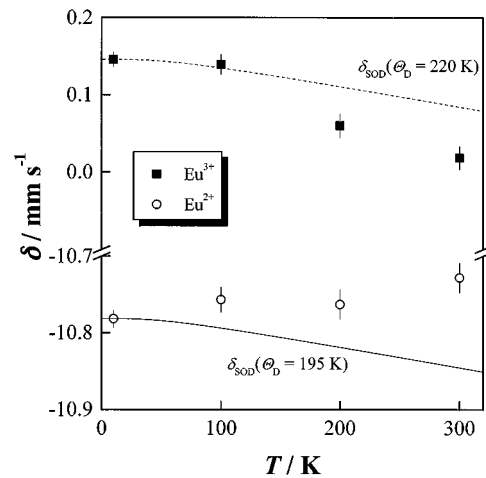

FIG. 5. Temperature dependence of the isomer shift of EuPd$_3$S$_4$; the solid line is the theoretical curve of the second-order Doppler (SOD) shift with $\Theta_D = 195$ K and the broken line is that of the SOD shift with $\Theta_D = 220$ K.

decrease with increasing temperature. We consider that these experimental results indicate the occurrence of an electron hopping between the Eu^{2+} and Eu^{3+} ions. An electron hopping between the Eu^{2+} and Eu^{3+} ions was observed in the ^{151}Eu Mössbauer spectra of a mixed valent europium sulfide Eu_3S_4 in which the Eu ions occupy one equivalent site (17, 18). The spectra of Eu_3S_4 consist of two absorption peaks for Eu^{2+} and Eu^{3+} at low temperatures. However, the two peaks become wider and approach each other at higher temperatures and the single peak forms at room temperature. In the spectrum of $EuPd_3S_4$ at 300 K, two sharp absorption peaks are observed as shown in Fig. 3. Thus, the activation energy for hopping in $EuPd_3S_4$ may be considerably higher than that of Eu_3S_4, and the electron hopping between the Eu^{2+} and Eu^{3+} ions below 300 K cannot be observed in time scale of the Mössbauer spectroscopic measurements in the case of $EuPd_3S_4$. $La_{0.5}Eu_{0.5}Pd_3S_4$ in which some Eu ions are substituted by La ions shows Mössbauer spectra similar to those of Eu_3S_4 and they are explained by the electron hopping model (M. Wakeshima and Y. Hinatsu, to be submitted). The spectra consist of two absorption peaks (the isomer shifts are -10.51 and -0.06 mm s^{-1}) for Eu^{2+} and Eu^{3+} ions at 10 K, the two absorption peaks become wider and approach each other with increasing temperature, and at 300 K only one broad peak ($\delta \sim -5.37$ mm s^{-1}) is observed. This result supports an electron hopping phenomenon between Eu^{2+} and Eu^{3+} in $EuPd_3S_4$. To determinate the activation energy of the electron hopping between Eu^{2+} and Eu^{3+}, Mössbauer spectrum measurements at higher temperatures are required.

Magnetic Properties

Figure 6 shows the magnetic susceptibilities of $EuPd_3S_4$ as a function of temperature at 0.1 T. This compound shows antiferromagnetic behavior below 3.0 K, which is lower than the transition temperature of $GdPd_3S_4$ ($T_N \sim 5.8$ K) (5). We consider that the dilution of the magnetic ions (Eu^{2+}) by the nonmagnetic ions (Eu^{3+}) results in a decrease of transition temperature. The ground state of Eu^{2+} ion ($^8S_{7/2}$) is the same as that of Gd^{3+} ion. The divergence between the ZFC and FC magnetic susceptibilities is not observed. The molar susceptibilities of $EuPd_3S_4$ is given by

$$\chi = n\chi(Eu^{3+}) + (1-n)\chi(Eu^{2+}) + \chi_0, \qquad [4]$$

where n is the molar ratio of Eu^{3+} in $EuPd_3S_4$, and χ_0 is the temperature-independent term containing the diamagnetic and Pauli paramagnetic term. The ground state of the Eu^{2+} ion is $^8S_{7/2}$ and hence the orbital angular momentum vanishes, and so the crystal field does not affect the Eu^{2+} compounds. The magnetic susceptibility of Eu^{2+} is represented by $N_A\mu_{eff}^2/3k(T - \Theta)$, where Θ is Weiss constant. The ground state of Eu^{3+} is nonmagnetic, and the excited states
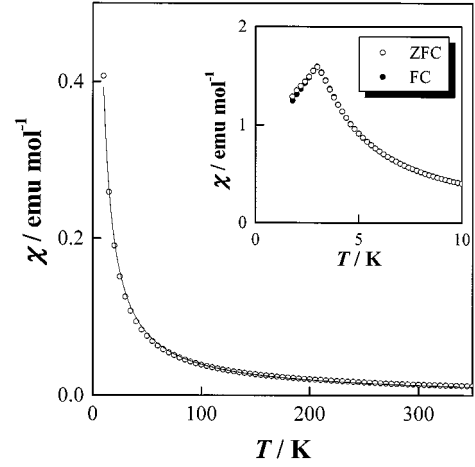

FIG. 6. Temperature dependence of the magnetic susceptibilities of $EuPd_3S_4$.

^7F_J ($J = 1, 2, \ldots, 6$) are close enough to give energy differences comparable to kT at room temperature. Thus, in consideration of the excited states, the magnetic susceptibility of Eu^{3+} can be written as (19),

$$\chi(Eu^{3+}) = \frac{N_A\mu_B^2/3k_B}{aT}$$
$$\times \frac{24 + (13.5a - 1.5)e^{-a} + (67.5a - 2.5)e^{-3a} + (189a - 3.5)e^{-6a} + \cdots}{1 + 3e^{-a} + 5e^{-3a} + 7e^{-6a} + \cdots},$$
$$[5]$$

where $a = \lambda/kT$ is 1/21 of the ratio of the over all multiplet width to kT. On the assumption that the screening number is 33, the theoretical value of λ is equal to 519 K (20). If λ and n were fixed to be 519 K and 50%, respectively, the values of μ_{eff} and Θ of Eu^{2+} were determined to be 7.58 μ_B and 1.0 K,
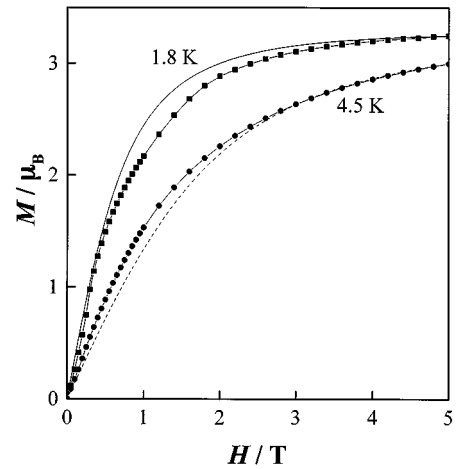

FIG. 7. Magnetization as a function of the magnetic field at 2 and 4.5 K for $EuPd_3S_4$; the solid line is the curve of the Brillouin function at 2 K and the broken line is that at 4.5 K.
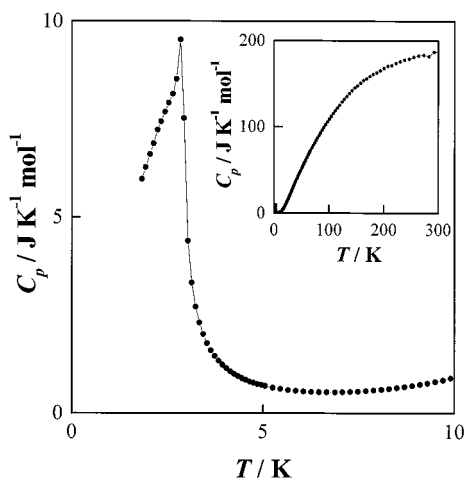
FIG. 8. Temperature dependence of the specific heat below 10 K for EuPd$_3$S$_4$; the inset shows the specific heat behavior between 2 and 300 K.

respectively, by fitting Eqs. [4] and [5] to the experimental data. The effective magnetic moment is slightly smaller than the theoretical one ($g\sqrt{S(S+1)} = 7.94\ \mu_B$).

Figure 7 shows the magnetization of EuPd$_3$S$_4$ as a function of applied magnetic field at 1.8 and 4.5 K. The solid and broken lines indicate the theoretical magnetization curves of the paramagnetic Eu^{2+} ion at 1.8 and 4.5 K, respectively. They are calculated from the relation $M = gSB_S(x)$ ($B_S(x)$ is a Brillouin function and $x = gS\mu_B H/kT$). The theoretical values are normalized so as to agree with the experimental values at 5 T. The magnetization curve at 1.8 K indicates an antiferromagnetic behavior with a weak magnetic exchange interaction and the antiferromagnetic state change to a ferromagnetic state without spin flip at higher fields because of a small magnetic anisotropy of the $^8S_{7/2}$ state. The saturated magnetic moment at 1.8 K ($M \sim 3.25\ \mu_B$ at 5 T) is slightly smaller than the expected one (3.5 μ_B).

The temperature dependence of the specific heat of EuPd$_3$S$_4$ is shown in Fig. 8. The sharp λ-type anomaly at 2.9 K indicates the existence of a long-range magnetic ordering. This magnetic ordering corresponds to the antiferromagnetic transition below 3 K observed from the magnetic susceptibility.

REFERENCE

1. D. A. Keszler and J. A. Ibers, *Inorg. Chem.* **22,** 3366 (1983).
2. D. A. Keszler, J. A. Ibers, and M. H. Mueller, *J. Chem. Soc. Dalton Trans.* 2369 (1985).
3. M. Wakeshima, T. Fujino, N. Sato, K. Yamada, and H. Masuda, *J. Solid State Chem.* **129,** 1 (1997).
4. N. Sato, M. Wakeshima, H. Masuda, K. Yamada, and T. Fujino, *High Temp.-High Pressures* **29,** 113 (1997).
5. M. Wakeshima and Y. Hinatsu, *J. Solid State Chem.* **146,** 226 (1999).
6. K. Abe, J. Kitagawa, N. Takeda, and M. Ishikawa, *Phys. Rev. Lett.* **83,** 5366 (1999).
7. J. Kitagawa, E. Matsuoka, N. Takeda, and M. Ishikawa, *Phys. Rev. B* **60,** R15028 (1999).
8. F. Izumi, *in* "The Rietveld Method" (R. A. Young, Ed.), Chap. 13. Oxford Univ. Press, Oxford, 1995.
9. C. K. Lowe-Ma, T. A. Vanderah, and T. E. Smith, *J. Solid State Chem.* **117,** 363 (1995).
10. D. L. Chess, C. A. Chess, and W. B. White, *Mater. Res. Bull.* **19,** 1551 (1984).
11. R. D. Shannon, *Acta Crystallogr. A* **32,** 751 (1976).
12. N. N. Greenwood and T. C. Gibb, "Mössbauer Spectroscopy." Plenum, New York, 1971.
13. O. Berkooz, *J. Phys. Chem. Solids* **30,** 1763 (1969).
14. U. F. Klein, G. Wortmann, and G. M. Kalvius, *J. Magn. Magn. Mater.* **3,** 50 (1976).
15. H. W. Wickman, M. Robbins, E. Buehler, and E. Catalano, *Phys. Lett. A* **31,** 59 (1970).
16. R. M. Housley and F. Hess, *Phys. Rev.* **146,** 517 (1966).
17. O. Berkooz, M. Malamud, and S. Shtrikman, *Solid State Commun.* **6,** 185 (1968).
18. B. C. Bunker, R. S. Drago, and M. K. Kroeger, *J. Am. Chem. Soc.* **104,** 4593 (1982).
19. J. H. Van Vleck, "The Theory of Electric and Magnetic Susceptibilities," p. 248. Clarendon, Oxford, 1932.